

First Principles Study of Structural and Elastic Properties of $BaWO_4$ Scheelite Phase Structure under Pressure

A. Benmakhlouf, A. Bentabet

Abstract—In this paper, we investigated the athermal pressure behavior of the structural and elastic properties of scheelite $BaWO_4$ phase up to 7 GPa using the ab initio pseudo-potential method. The calculated lattice parameters pressure relation have been compared with the experimental values and found to be in good agreement with these results. Moreover, we present for the first time the investigation of the elastic properties of this compound using the density functional perturbation theory (DFPT). It is shown that this phase is mechanically stable up to 7 GPa after analyzing the calculated elastic constants. Other relevant quantities such as bulk modulus, pressure derivative of bulk modulus, shear modulus; Young's modulus, Poisson's ratio, anisotropy factors, Debye temperature and sound velocity have been calculated. The obtained results, which are reported for the first time to the best of the author's knowledge, can facilitate assessment of possible applications of the title material.

Keywords—Pseudo-potential method, pressure, structural and elastic properties, scheelite $BaWO_4$ phase.

I. INTRODUCTION

BOTH $CaWO_4$ and $PbWO_4$ are promising materials for the next generation of cryogenic phonon-scintillation detectors [1]-[3]. This has motivated a renewed interest on the fundamental physical properties of the AWO_4 tungstates (with $A = Ca, Sr, Ba, Pb, Eu$) which under normal conditions crystallize in the tetragonal scheelite structure [4].

The scheelite tungstates are in fact technologically important materials used during the last years as solid-state scintillators [5]-[7] and in other optoelectronic devices [8]-[10]. In the last few years, the barium tungstate $BaWO_4$, crystal with a Scheelite structure, has attracted interests of several research groups due to his applications as laser host material, scintillator in high-energy physics detectors and oxide ion conductor [11]. Among the tungstate materials, $BaWO_4$ is a potential material to be a universal Raman-active crystal [12]-[14]. Structurally, under compression, $BaWO_4$ exists in several forms, such as scheelite, wolframite, fergusonite and $HgMoO_4$ [15]-[17]. At ambient conditions up to 7GPa, it's known to exist in the scheelite structure, Fig. 1. The scheelite crystal structure is characterized by the tetragonal space group $I4_1/a$ listed as No. 88 in the International Tables of Crystallography, with a number of

formula units per cell $Z=4$ [4]. In this structure, the primitive unit cell has two ABX_4 units. The scheelite crystal structure can be described as highly ionic with A^{+2} cations and tetrahedral BX_4^{-2} anions. Each B site is surrounded by four equivalent X sites in tetrahedral symmetry and the tetrahedral BX_4^{-2} anions have short B-X bond lengths, which are quite rigid even under compression [18].

The goal of the present study is to examine comprehensively the effect of pressure on the structural and elastic properties of the scheelite crystal $BaWO_4$ up to 7GPa in order to help understand and control the material properties under stress. The rest of the paper has been divided in three parts. In Section II, we briefly describe the computational techniques used in this study. The most relevant results obtained for the structural and elastic properties of the $BaWO_4$ crystal are presented and discussed in Section III. Finally, in Section IV we summarized the main conclusions of our work.

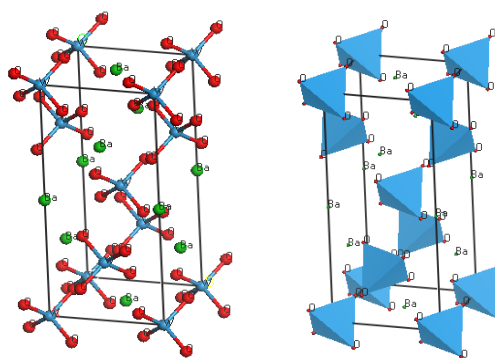


Fig. 1 $1 \times 1 \times 1$ Unit cell of $BaWO_4$ tetragonal structure (scheelite) at ambient conditions). The W atoms are tetrahedrally coordinated to oxygen

II. COMPUTATIONAL METHOD

Theoretical calculations were performed by employing pseudo-potential plane-wave (PP-PW) method as implemented in the CASTEP (Cambridge Serial Total Energy Package) code [19]. Interactions of valence electrons with ion cores were represented by the Vanderbilt-type ultra-soft pseudo-potential [20]. The exchange-correlation potential was calculated by the generalized gradient approximation (GGA) based on Perdew Wang (PW91) [21]. The PW91 is widely used in DFT. Moreover, several density functions, such as PBE, RPBE and LDA, have been tested in the calculations of electronic structures and optical properties for the $PbWO_4$ and $CaMoO_4$ crystal. The calculated results using the PW91 are more close to the experimental results. The structure of

A. Benmakhlouf is with the Département de Physique, Faculté des Sciences Exactes, université Abderrahmane Mira – Bejaia, Algérie and is with the Laboratoire de Physique des Matériaux, Université Amar Telidji de Laghouat; BP 37G, Laghouat 03000, Algérie (corresponding author to provide phone: 0555153835; e-mail: benmakhlouf_ab@yahoo.fr).

A. Bentabet is with Laboratoire de Recherche : Caractérisation et Valorisation des Ressources Naturelles, Université de Bordj Bou Arreridj, 34000, Algérie.

$BaWO_4$ is similar to $PbWO_4$ and $CaMoO_4$ crystal [12]. So they must be the similar properties and the PW91 is selected in this paper. In addition, there are many successful calculations using PW91 [22], [23].

To ensure highly converged and precise results, the integration over the Brillouin zone was done over a $6 \times 6 \times 4$ Monkhorst–Pack grid [24]; the kinetic energy cutoff was set to 700 eV. The equilibrium lattice constant and positional parameters are determined from the global minimum energy. The structural parameters were determined using Broyden–Fletcher–Goldfarb–Shanno (BFGS) minimization technique [25]. The self-consistent calculations are considered to be converged when the total energy of the system is stable within 5×10^{-7} eV/atom.

III. RESULTS AND DISCUSSION

A. Equilibrium Structural and Elastic Properties

In this work, the initial crystal structure has been built based on the experimental crystallographic data of scheelite phase [26]. To optimize the geometry structure, the ions were relaxed until the Hellman–Feynman forces were below 0.01 eV \AA^{-1} and the cell parameters were relaxed until total stresses were below 0.02 GPa. The calculated equilibrium lattice parameters are shown in Table I along with the available experimental and theoretical values for comparison. Our obtained results are in good agreement with the corresponding measured one. The relative differences between the calculated and experimental values of the lattice parameters $d(\%) = (\text{calculated value} - \text{measured value}) / (\text{measured value})$ are smaller than $\mp 1.4\%$. This good agreement serves as a proof of reliability and accuracy of the used theoretical method.

TABLE I
CALCULATED LATTICE PARAMETERS (a_0, c_0 , in \AA), UNIT CELL VOLUME (V , in \AA^3), BULK MODULUS (B_0 , in GPa) BY MEANS OF VRH APPROXIMATION AND THE FIRST PRESSURE DERIVATIVE OF THE BULK MODULUS B'_0 OF $BaWO_4$ SCHEELITE PHASE STRUCTURE, AT ZERO PRESSURE, COMPARED WITH PREVIOUS STUDIES

This work	Exp. [15]	Exp. [16]	Exp. [17]	Exp. [26]
5.69	5.63	5.61	5.61	5.61
12.84	12.75	12.8	12.72	12.71
415.19	404.13	402.84	400.32	400.01
56.28	57.00	52.00	47.00	
4.76	3.50	5.00	4.00	

The elastic parameters determine the response of the crystal to external forces, as characterized by elastic stiffness coefficients C_{ij} , bulk modulus B , shear modulus G , Young's modulus E and Poisson's ratio ν , and obviously play an important part in determining the strength of the materials. The values of elastic parameters provide valuable information about the bonding characteristic between adjacent atomic planes and the anisotropic character of the bonding and structural stability [27], [28]. The linear elastic constants form a 6×6 symmetric matrix, having 27 different components. Any symmetry present in the structure may make some of these components equal and others may be fixed at zero. Thus, a

tetragonal crystal has seven different symmetry elements ($c_{11}, c_{33}, c_{44}, c_{66}, c_{12}, c_{13}$ and c_{16}). The complete sets of zero-pressure single crystal elastic constants were calculated by using strain-stress method [29]. Table II shows the calculated full set elastic constants of $BaWO_4$. We are not aware of any experimental data. We consider the present elastic constants as a prediction study for this crystal. The elastic stability is a necessary condition for a stable crystal. A tetragonal crystal has to obey the following restrictions of its elastic constants [30]:

$$C_{11} > 0, C_{33} > 0, C_{44} > 0, C_{66} > 0, C_{11} - C_{12} > 0, C_{11} + C_{33} - 2C_{13} > 0, 2(C_{11} + C_{12}) + C_{33} + 4C_{13} > 0 \quad (1)$$

In terms of the above conditions, the calculated elastic constants (Table II) indicate that $BaWO_4$ scheelite structure is mechanically stable at zero pressure.

The elastic constants C_{11} and C_{33} determine the resistance to linear compression in the (a, b) and c directions, respectively. The calculated C_{33} for $BaWO_4$ is lower than C_{11} . Thus, the c axis is more compressible than a and b axis. The C_{44} measures the shear elastic modulus along the [010] direction on the (001) plane and the C_{66} represents the shear elastic modulus along the [100] direction on the (010) plane [31]. The calculated C_{44} and C_{66} are 26.87 and 32.86 respectively. These small values mean a low resistance to the monoclinic shear distortion.

TABLE II
ELASTIC CONSTANTS C_{ij} [IN GPa] OF $BaWO_4$ TETRAGONAL STRUCTURE AT ZERO PRESSURE

C_{11}	C_{33}	C_{44}	C_{66}	C_{12}	C_{13}	C_{16}
89,66	78,91	26,87	32,86	46,4	39,45	9,96

Like the elastic constant tensor, the macroscopic elastic parameters, bulk modulus B and shear modulus G , contain information regarding the hardness of a material with respect to various types of deformation. The bulk modulus is much more facile to determine experimentally (by using Birch–Murnaghan equation [32]) than the elastic constant tensor. Alternatively, the bulk and shear moduli are also related to the elements of the elastic constant via the Voigt-Reus–Hill approach [33]–[35]. Table I provides the calculated Bulk modulus B_0 at zero pressure along with available experimental data. Our results are in a good agreement with values given by experience. The Young's modulus E , which measures the stress strain ratio in the case of tensile forces and the Poisson's ratio ν , which is defined as the negative value of lateral (or transverse) strain to the longitudinal strain under uniaxial stress and no volume change [36], are given by [31].

$$E = \frac{9B_0G}{3B_0 + G} \quad (2)$$

$$\nu = \frac{3B_0 - 2G}{2(3B_0 + G)} \quad (3)$$

The obtained values of the above-mentioned macroscopic elastic parameters are listed in Table III.

The ratio of bulk modulus to shear modulus, B_0/G , is proposed as a criterion to distinguish between ductile and brittle characters of a solid. According to the empirical formula of Pugh [37], a material is brittle (ductile) if the B_0/G ratio is less (greater) than 1.75. The obtained value of the B_0/G ratio in the present work is equal to 2.24, which predicts $BaWO_4$ to be a ductile material.

The value of Poisson's ratio is indicative of the degree of directionality of the covalent bonds. This value is small ($\nu = 0.1$) for covalent materials, whereas for the ionic materials a typical value of ν is 0.25 [31]. As shown in Table III, the calculated Poisson's ratio is about 0.30 for $BaWO_4$. Therefore, the ionic contribution to the interatomic bonding for this compound is dominant, which agree with the results given in references [18], [38], [39].

The shear anisotropic factors in different crystallographic planes provide a measure of the degree of anisotropy of atomic bonding in different planes. A value of unity means that the crystal exhibits isotropic properties while values other than unity represent varying degrees of anisotropy. From the elastic constants, we obtain the shear anisotropic factors given for a tetragonal structure by [31].

$$A_1 = A_2 = \frac{4C_{44}}{c_{11} + c_{33} - 2c_{13}} ; \quad A_3 = \frac{2C_{66}}{c_{11} - c_{13}} \quad (4)$$

For the (100), (010) and (001) planes, respectively. The calculated vales are as follows: $A_1 = A_2 = 1,20$, and $A_3 = 1,31$, this indicates that the elastic properties of the structure are highly anisotropic in the 3 directions.

TABLE III

CALCULATED BULK, SHEAR AND YOUNG'S MODULI (B, G and E , in GPa), POISSON'S RATIO ν AND B_0/G RATIO OF THE $BaWO_4$ SCHEELITE STRUCTURE AT ZERO PRESSURE. THE SUBSCRIPT V, R AND 0 REFER TO THE VOIGT, REUSS AND HILL APPROXIMATIONS, RESPECTIVELY

	B			G			E	ν	B_0/G
	B_V	B_R	B_0	G_V	G_R	G_0			
BaWO₄	56.54	56.03	56.28	26.18	24.03	25.11	65.58	0.30	2.24

Once we have calculated the bulk modulus, the shear modulus G and the Young's modulus E , we may obtain the Debye temperature, which is an important fundamental parameter closely related to many physical properties such as specific heat and melting temperature. At low temperatures the vibrational excitations arise solely from acoustic vibrations. Hence, at low temperature the Debye temperature calculated from elastic constants is the same as that determined from specific heat measurements. We have calculated the Debye temperature (θ_D) based on the elastic constants using the following common relation [40].

$$\theta_D = \frac{h}{k_B} \left[\frac{3n}{4\pi} \left(\frac{N_A \rho}{M} \right) \right]^{1/3} v_m \quad (5)$$

here, h is the Plank's constant, K_B is the Boltzmann's constant, n is the number of atoms per molecule ($n=4$ for $KAlQ_2$), N_A is the Avogadro's number, M is the molecular weight, $\rho = M/V$ is the density of mass and v_m is the average sound velocity given by [41].

$$v_m = \left[\frac{1}{3} \left(\frac{2}{v_l^2} + \frac{1}{v_t^2} \right) \right]^{-1/3} \quad (6)$$

where v_l and v_t are the longitudinal and transverse elastic wave velocities, respectively. They can be obtained from Navier's equations [40].

$$v_l = \sqrt{\frac{3B_0 + 4G_0}{3\rho}}, \quad v_t = \sqrt{\frac{G_0}{\rho}} \quad (7)$$

The calculated sound velocities and Debye temperature as well as the density of $BaWO_4$ scheelite structure at zero pressure are given in Table IV. Unfortunately, there are no theoretical and experimental results to be compared with them.

TABLE IV

CALCULATED DENSITY ρ (in Mg/m^3), LONGITUDINAL, TRANSVERSE AND AVERAGE SOUND VELOCITY (v_l, v_t, v_m , respectively, in ms^{-1}) AND DEBYE TEMPERATURE (θ_D , in K) FOR THE $BaWO_4$ SCHEELITE STRUCTURE AT ZERO PRESSURE

	v_l	v_t	v_m	θ_D	ρ
BaWO₄	3021.51	2018.23	2205.77	253.99	6.16

B. Structural and Elastic Properties under Pressure

In order to show how to behave the structural parameters under pressure, the equilibrium geometries of $BaWO_4$ scheelite structure unit cell were computed at fixed values of applied hydrostatic pressure in the range from 0 to 7 GPa , where, at each pressure, a complete optimization for lattice constants is performed. Pressure dependence of the lattice parameters is shown in Fig. 2. We clearly observe a quadratic dependence in all curves of this compound in the considered range of pressure. The solid curve is quadratic least squares fit. The values of linear and quadratic pressure coefficients for the lattice parameter of this structure are given in Table VI together with experimental results of other authors. The present results agree well with the previous experimental values reports for this material [15]. This result shows the power of this method to describe the behavior of a structure under pressure and gives confidence in the predicted results.

TABLE V

CALCULATED LINEAR AND QUADRATIC PRESSURE COEFFICIENTS OF THE LATTICE PARAMETERS A (P), C (P) OF $BaWO_4$ SCHEELITE STRUCTURE

	a_0	a_1	a_2	c_0	c_1	c_2
This work	5,68574	-	9,429 $\times 10^{-4}$	12,842	-	19,10 $\times 10^{-4}$
Exp.[15]	5,6257	-	6,929 $\times 10^{-4}$	12,749	-	20,02 $\times 10^{-4}$

Pressure dependences of the normalized lattice parameters (a/a_0 and c/c_0), normalized unit cell volume (V/V_0) (where a_0 , c_0 and V_0 are zero pressure equilibrium structure parameters) are illustrated in Fig. 3.

It is shown that, as pressure increases, the normalized lattice parameter c/c_0 decreases more rapidly than the normalized lattice parameters a/a_0 , which indicates that the c-axis is more compressible than the a- and b-axes. These results implicate that the atomic bonds along the a- and b-directions between nearest neighbors are stronger than those along the c-direction.

As it is shown in Fig. 3, the volume of the unit cell decreases about at 9% and at 7 GPa of its initial value at zero pressure.

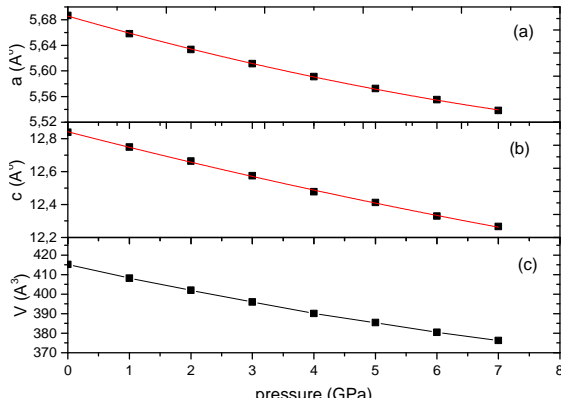


Fig. 2 (a) The lattice constant pressure relation (a–P); the solid line is a quadratic least squares fit: $a(p) = a_0 + a_1 p + a_2 p^2$; (b) The lattice constant pressure relation (c–P); the solid line is a quadratic least squares fit: $c(p) = c_0 + c_1 p + c_2 p^2$. (c) Evolution of volume under pressure

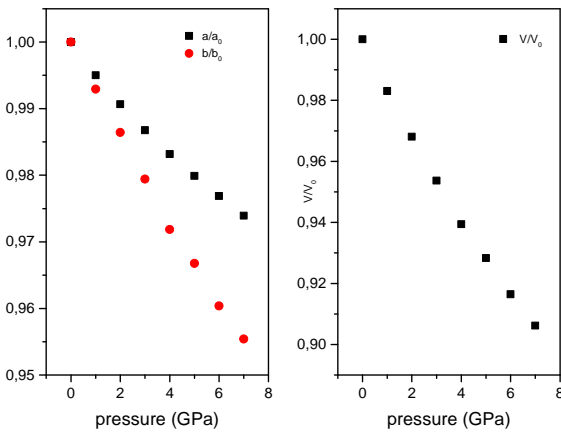


Fig. 3 Pressure dependence of the normalized lattice constants (a/a_0 and c/c_0), normalized unit cell volume (V/V_0) (where a_0 , c_0 and V_0 are zero pressure equilibrium structure parameters) in $BaWO_4$ Scheelite phase

From the present work, we further obtain information on bond compressibility (see Fig. 4). In particular, under hydrostatic conditions, the W-O short distance is 7% less compressible than the Ba-O distance. A similar qualitative behavior is found by [17] which gives the value of 10%. For scheelite $BaWO_4$ structure, the first neighbor W-O distances is more rigid than the Ba-O ones. As a consequence, the volume change of BaO8 dodecahedra is larger than that of WO4 tetrahedra.

Now we are interested to study the pressure dependence of the elastic properties. The first principle studies based on DFT can be used to obtain reliable elastic properties of compounds. Several methods are available for computation of stiffness coefficients, but currently the ‘stress–strain’ method seems to be most commonly used and this is the method implemented in CASTEP. In this approach, the ground state structure is

strained according to symmetry dependent strain patterns with varying amplitudes and a subsequent computing of the stress tensor after a re-optimization of the internal structure parameters, i.e., after a geometry optimization with fixed cell parameters. The elastic stiffness coefficients are then the proportionality coefficients relating the applied stress to the computed strain [42].

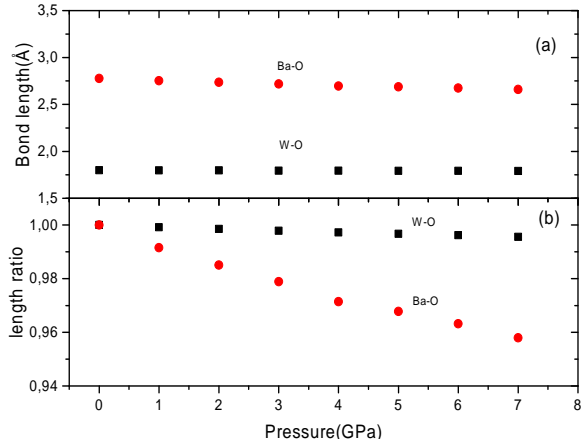


Fig. 4 Pressure dependence of the interatomic bond distances (a) and bond length ratio Ba-O and W-O (b) in the Scheelite phase structure $BaWO_4$

In Fig. 5, we present the variation of the elastic constants (C_{ij}), the bulk modulus B , the shear modulus G and the Born’s criteria for tetragonal crystal [30] of $BaWO_4$ in scheelite phase, with respect to the variation of pressure. We clearly observe a linear dependence in all curves of elastic constants and bulk modulus of this crystal in the considered range of pressure. In Table VI, we listed our results for the pressure derivatives $\partial C_{ij}/\partial P$ and $\partial B/\partial P$. It is easy to observe that the elastic constants C_{ij} increase when the pressure is enhanced in this crystal, and satisfy the Born’s criteria (Fig. 5 (c)) indicating that scheelite phase $BaWO_4$ compound is mechanically stable up to 7 GPa. This result is confirmed by other experimental ones [15]–[17]. The calculated pressure derivative $B' = \partial B/\partial P$ is given in Table I with other theoretical and experimental data for comparison. The results of our work agree well with the previous theoretical and experimental reports for this material. To our knowledge, no experimental or theoretical data for the pressure derivative of elastic constants of these compounds are given in the literature. Then, our results can serve as a prediction for future investigations.

$\frac{\partial C_{11}}{\partial P}$	$\frac{\partial C_{33}}{\partial P}$	$\frac{\partial C_{44}}{\partial P}$	$\frac{\partial C_{66}}{\partial P}$	$\frac{\partial C_{12}}{\partial P}$	$\frac{\partial C_{13}}{\partial P}$	$\frac{\partial C_{16}}{\partial P}$	$\frac{\partial B}{\partial P}$
5,693	3,955	0,6956	2,41262	5,83548	4,30595	0,72774	4,76255

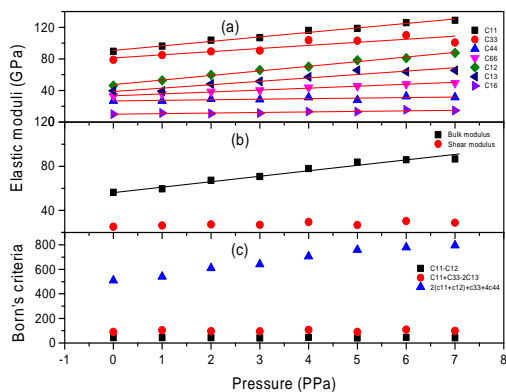


Fig. 5 Calculated pressure dependence of: (a) elastic constants (C_{ij}), (b) bulk and shear moduli and (c) the Born's criteria for the tetragonal $BaWO_4$ structure: The solid line is a linear fit

IV. CONCLUSION

We have investigated the structural and elastic properties of the $BaWO_4$ scheelite phase structure under pressure. The calculations are done by the generalized gradient approximation (GGA) potential of Perdew Wang (PW91). A summary of our results follows.

- The calculated structural parameters at ambient pressure of this compound are in a good agreement with the available experimental and theoretical data, validating the method used in present work.
- The elastic constants, Debye temperature and sound velocity are calculated at zero pressure for the $BaWO_4$ scheelite compound.
- Our calculated results for the pressure dependence of the structural parameters shows a quadratic dependence in all curve of this compound in the considered range of pressure.
- For scheelite $BaWO_4$ structure, the first neighbor W-O distances is more rigid than the Ba-O ones.
- We have found a linear dependence of bulk modulus and elastic constants with applied pressure.
- We are not aware of any experimental or theoretical data for the elastic constants and pressure dependence of this compound, so our results may be considered as reliable predictions of the pressure dependence of the elastic properties in this material.

REFERENCES

- G. Angloher, M. Bruckmayer, C. Bucci, M. Bühler, S. Cooper, C. Cozzini, P. Di Stefano, F. V. Feilitzsch, T. Frank, D. Hauff, T. Jagemann, J. Jochum, V. Jorgens, R. Keeling, H. Kraus, M. Loidl, J. Marchese, O. Meier, U. Ángel, F. Pröbst, Y. Ramachers, A. Rulofs, J. Schnagl, W. Seidel, I. Sergeev, M. Sisti, M. Stark, S. Uchaikin, L. Stodolsky, H. Wulandari, and L. Zerle, *Astroparticle Physics* 18 (2002) 43.
- G. Angloher, C. Bucci, C. Cozzini, F. von Feilitzsch, T. Frank, D. Hauff, S. Henry, T. Jagemann, J. Jochum, H. Kraus, B. Majorovits, J. Ninkovic, F. Petricca, F. Probst, Y. Ramachers, W. Rau, W. Seidel, M. Stark, S. Uchaikin, L. Stodolsky, and H. Wulandari, *Nucl. Instrum. Methods Phys. Res. A* 520 (2004) 108.
- S. Cebrian, N. Coron, G. Dambier, E. García, I. G. Irastorza, J. Leblanc, P. de Marcillac, A. Morales, J. Morales, A. Ortiz de Solórzano, J. Puimedon, M. L. Sarsa, and J. A. Villar, *Astroparticle Physics* 21 (2004) 23.
- A. W. Sleight, *Acta Cryst. B* 28 (1972) 2899.
- A. A. Annenkov, M. V. Korzhik, and P. Lecoq, *Nucl. Instrum. Methods Phys. Res. A* 490 (2002) 30.
- Compact Muon Solenoid (CMS), Technical Proposal, CERN/LHC 93 - 98, p. 1(1994).
- M. Kobayashi, M. Ishi, Y. Usuki, H. Yahagi, *Nucl. Instrum. Methods Phys. Res. A* 333 (1993) 429.
- M. Nikl, P. Bohacek, N. Mihokova, M. Kobayashi, M. Ishii, Y. Usuki, V. Babin, A. Stolovich, S. Zazubovich, and M. Bacci, *J. of Luminescence* 1136 (2000) 87.
- M. Nikl, P. Bohacek, N. Mihokova, N. Solovieva, A. Vedda, M. Martini, G. P. Pazzi, P. Fabeni, M. Kobayashi, M. Ishii, *J. Appl. Phys.* 91 (2002) 5041.
- A. Brenier, G. Jia, and Ch. Tu, *J. Phys.: Condens. Matter* 16, 9103 (2004).
- C. Zhang, X.Y. Zhang, Q.P. Wang, S.Z. Fan, X.H. Chen, Z.H. Cong, Z.J. Liu, Z. Zhang, H.J. Zhang, and F.F. Su, *Laser Phys. Lett.* 6, 7 (2009) 505.
- Haiyan Zhang, Tingyu Liu, Qiren Zhang, Xi'en Wang, Xiaofeng Guo, Min Song, Jigang Yin, *Physica B* 404 (2009) 1538.
- P. C 'erny', P.G. Zverev, H. Jeli 'nkova', T.T. Basiev, *Optics Communications* 177 (2000) 397.
- W.W. Ge, H.J. Zhang, J.Y. Wang, J.H. Liu, X.G. Xu, X.B. Hu, M.H. Jiang, D.G. Ran, S.Q. Sun, H.R. Xia, R.I. Boughton, *Journal of Applied Physics* 98 (2005) 013542.
- V. Panchal, N. Garg, A.K. Chauhan, Sangeeta, S. M. Sharma, *Solid state Communications* 130 (2004) 203.
- D. Errandonea, J. Pellicer-Porres, F. J. Manjón, A. Segura, Ch. Ferrer-Roca, R. S. Kumar, O. Tschauner, J. López-Solano, P. Rodríguez-Hernández, S. Radescu, A. Mujica, A. Muñoz, and G. Aquilanti, *Physical Review B* 73 (2006) 224103.
- O. Gomis, J. A. Sans, R. Lacomba-Perales, D. Errandonea, Y. Meng, J. C. Chervin, and A. Polian, *Phys. Rev. B* 86 (2012) 054121.
- D. Errandonea and Francisco Javier Manjón, To appear in *Progress in Materials Sciences* (2008).
- S.J. Clark, M.D. Segall, C.J. Pickard, P.J. Hasnip, M.J. Probert, K. Refson, M.C. Payne, *Zeitschrift für Kristallographie* 220 (2005) 567.
- D. Vanderbilt, *Phys. Rev. B* 41 (1990) 7892.
- J. P. Perdew, J.A. Chevary, S.H. Vosko, K.A. Jackson, M.R. Pederson, D.J. Singh and C. Fiolhais, *Phys. Rev. B* 46 (1992) 6671.
- P. P. Rushton, S.J. Clark, D.J. Tozer, *Physical Review B* 63 (2001) 115206.
- Y. Yamaguchi, K. Tabata, T. Yashima, *Journal of Molecular Structure: Theochem* 714 (2005) 221.
- H.J. Monkhorst, J.D. Pack, *Phys. Rev. B* 13 (1976) 5188.
- T.H. Fischer, J. Almlof, *J. Phys. Chem.* 96 (1992) 9768.
- L.S. Cavalcante et al. *Journal of Alloys and Compounds* 474 (2009) 195.
- E. Schreiber, O. L. Anderson and N.Soga. *Elastic Constants and their Measurement* (New York: McGraw-Hill) (1973).
- J.F. Nye. *Physical Properties of Crystals* (Oxford: Oxford Science Publications) (1957).
- V. Milman, M.C. Warren, *J. Phys.: Condens. Matter* 13 (2001) 241.
- D.C. Wallace, *Thermodynamics of Crystal*, Wiley, New York, (1972) (Chapter 1).
- A. Yildirim, H. Koc and E. Deligoz, *Chin. Phys. B* Vol. 21, No. 3 (2012) 037101.
- F. Birch, *Phys. Rev* 71 (1947) 809.
- W. Voigt, *Lehrbuch der Kristallphysik*, Verlag und Druck, Von BG Teubner, in Leipzig und Berlin, (1928).
- A. Reuss, *Z. Angew. Math. Mech.* 9 (1929) 49.
- R. Hill, *Proc. Phys. Soc. London* 65 (1952) 349.
- O. Boudrifa, A. Bouhemadou, N. Guechi, S. Bin-Omran, Y. Al-Douri, R. Khenata, *Journal of Alloys and Compounds* 618 (2015) 84.
- S. F. Pugh, *Philos. Mag.* 45 (1954) 823.
- E. F. Paski, and M. W. Blades, *Anal. Chem.* 60 (1988) 1224.
- S. Takai, K. Sugiura, and T. Esaka, *Mater. Res. Bull.* 34 (1999) 193.
- O. L. Anderson, *J. Phys. Chem. Solids* 24 (1963) 909.
- E. Schreiber, O.L. Anderson and N.Soga. *Elastic Constants and Their Measurements* (New York: McGraw-Hill) (1973).
- A. Bouhemadou, R. Khenata, *Physics Letters A* 360 (2006) 339.